Economical Determination of Departure Points for Semi-Lagrangian Models

JOHN L. MCGREGOR

CSIRO, Division of Atmospheric Research, Mordialloc, Victoria, Australia

(Manuscript received 11 September 1991, in final form 13 February 1992)

ABSTRACT

An Eulerian procedure that avoids both interpolation and iteration is proposed for determining the departure points of trajectories. It is applicable to semi-Lagrangian models formulated either on the plane or on the sphere. The technique can achieve a high degree of accuracy; it is also simpler and more economical than other schemes, especially when applied on the sphere. The technique is applied to the cone advection test on the plane, as well as to a "Gaussian hill" problem on a rotating sphere.

1. Introduction

During the last 10 years, there has been increasing interest in semi-Lagrangian techniques for handling horizontal or vertical advection in numerical weather prediction models (e.g., Robert 1981, 1982; Bates and McDonald 1982; McDonald 1986; McGregor 1987; Ritchie 1987; Tanguay et al. 1989). The essential feature of such schemes is that the total or material derivatives in the equations of motion are handled directly by calculating the departure points of fluid parcels; the upstream value of the required fields are then usually evaluated by spatial interpolation. The popularity of the semi-Lagrangian approach stems not only from the large permissible time steps, but also from the high degree of advection accuracy. The schemes may be either two time level or three time level.

This paper describes an alternative method for determining the position of the departure points. A simple straight-line trajectory back in time using just the velocity at the arrival point possesses inadequate accuracy; this was realized by Robert (1982). Presently, the most popular schemes involve a sequence of iterations: a first guess of the departure position is determined as just described; an estimate of departure velocity is found by horizontal interpolation at the midpoint of the trajectory; the process is repeated several times using an updated advection velocity (e.g., Temperton and Staniforth 1987; McDonald 1987; Ritchie 1987; McDonald and Bates 1987, 1989). A significant overhead of such schemes can arise from the horizontal interpolations (traditionally bicubic) carried out during the iterations, although McDonald (1987) has shown that lower-order interpolations can be used for the early iterations; it should also be noted that Staniforth and Pudykiewicz (1985), Temperton and Staniforth (1987), and Bates et al. (1990) report acceptable accuracy using just linear interpolation. The computational overheads of the interpolations are greater in the case of a spherical domain (Ritchie 1987; Williamson and Rasch 1989; McDonald and Bates 1989).

The present scheme, as described in section 2, avoids this horizontal interpolation in the trajectory calculations. This paper does not address the overheads of the final interpolations needed to update the fields themselves. An operation count is provided in section 2, as is an error analysis. Equations are also given for applying the scheme on the sphere. Section 3 presents an application to the cone advection test. Section 4 applies the scheme to steady solid-body rotation of a "Gaussian hill" on a sphere, a problem suggested by Ritchie (1987). Section 5 provides some concluding comments.

2. Theory

a. Derivation of the new scheme

Let $\mathbf{r}(t)$ denote a member of a set of vectors moving with the fluid where each vector will be associated at time t with a different grid point; note that the vectors move with the fluid, although the grid points themselves have fixed locations. To advance the model integration from time τ to $\tau + \Delta t$, a vector $\mathbf{r}(\tau + \Delta t)$ is set up at the position of each arrival grid point. It is required to find the starting position of the vector at the preceding time step, namely, $\mathbf{r}(\tau)$. This may be expressed in terms of a truncated Taylor series

$$\mathbf{r}(\tau) \approx \mathbf{r}(\tau + \Delta t) + \sum_{n=1}^{N} \frac{(-\Delta t)^n}{n!} \frac{d^n \mathbf{r}}{dt^n}(\tau + \Delta t), \quad (1)$$

Corresponding author address: Dr. John L. McGregor, CSIRO, Division of Atmospheric Research, PMB No. 1 Mordialloc, Victoria 3195, Australia.

where

$$\frac{d^n\mathbf{r}(t)}{dt^n} = \frac{d}{dt}\left[\frac{d^{n-1}\mathbf{r}(t)}{dt^{n-1}}\right] \quad n = 2, 3, \cdots, N, \quad (2)$$

and the total derivative operator has the usual definition of time derivative following the motion of a parcel,

$$\frac{d}{dt} = \frac{\partial}{\partial t} + \mathbf{v}\cdot\nabla. \quad (3)$$

An array of the vectors $\mathbf{r}(\tau + \Delta t)$ is needed in order that the $\mathbf{v}\cdot\nabla$ operator in (3) may be conveniently evaluated; $\mathbf{v} = d\mathbf{r}/dt$ is the velocity of the fluid at position $\mathbf{r}(t)$, and ∇ is the spatial gradient operator. In (3), the time derivative on the left-hand side (lhs) is naturally viewed in a Lagrangian sense. The right-hand side (rhs) allows its instantaneous evaluation at the same point in time and space via Eulerian derivatives. If desired (e.g., during coordinate transformations), (3) can be consistently applied to give an Eulerian evaluation of $d\mathbf{r}/dt$; in this case the rhs reduces just to the velocity because $\partial\mathbf{r}/\partial t$ is identically zero from the independence of space and time coordinates for partial derivatives (by definition).

In the above equations, it can be seen that each component of $\mathbf{r}$ may be obtained independently of the others. If desired, the velocities and the scalar gradient operator $\mathbf{v}\cdot\nabla$ in (3) may be expressed in quite different coordinates from those specifying $\mathbf{r}$. This option proves particularly useful in the context of modeling advection on a sphere, where $\mathbf{r}$ is assigned in Cartesian coordinates, while $\mathbf{v}\cdot\nabla$ may be applied in polar form separately to each Cartesian component.

If the Eulerian velocities change with time, it becomes difficult, or at least very cumbersome, to evaluate the partial time derivatives for the higher-order terms at $\tau + \Delta t$. The scheme proposed in the present paper replaces the total time derivative in (3), for use in (1) and (2), by the approximate formula

$$\frac{d}{dt} \approx \hat{\mathbf{v}}\cdot\nabla. \quad (4)$$

Here $\hat{\mathbf{v}}$ represents the (Eulerian) velocity at the point in space corresponding to $\mathbf{r}(\tau + \Delta t)$, but evaluated at the intermediate time $\tau + \Delta t/2$. The above scheme using (1), (2), (4), and retaining terms up to the Nth total time derivative will be called a D_N scheme. The velocity $\hat{\mathbf{v}}$ may be conveniently determined by means of extrapolation in time from the known velocities at previous time steps; a formula with third-order accuracy in time was suggested by Temperton and Staniforth (1987):

$$\hat{\mathbf{v}} = 1/8\,[15\mathbf{v}(\tau) - 10\mathbf{v}(\tau - \Delta t) + 3\mathbf{v}(\tau - 2\Delta t)] + O(\Delta t^3). \quad (5)$$

The idea behind the approximation (4) is that for advection purposes the velocities are considered to remain constant in an Eulerian sense over the time interval $(\tau, \tau + \Delta t)$ at their centered-in-time value. Although it is not explicitly stated, this same approximation is effectively made in most recent centered-in-time semi-Lagrangian schemes in that they use only $\hat{\mathbf{v}}$ velocity information for determining departure points; an exception is a higher-order time scheme proposed by McDonald (1987). Equation (4) shows that the lowest-order D_1 scheme just produces a straight-line trajectory using a velocity $\hat{\mathbf{v}}$ evaluated at the arrival position. The D_2 scheme uses estimates for both the velocity and acceleration along the trajectory. Mathur (1970) also used the fluid velocity and acceleration in calculating his departure points in a relatively complicated iterative procedure; the comparative accuracy of his scheme is not readily apparent. The D_3 and higher-order versions of the scheme effectively solve for the trajectory by incorporating higher-order curvature terms derived kinematically for the arrival point from the velocity field $\hat{\mathbf{v}}$ valid at time $\tau + \Delta t/2$.

It should be noted that the test calculations shown in this paper will be carried out only for velocities that remain constant with time, although the error analysis provides guidance for the more general case, and the scheme has been successfully incorporated into a full limited-area primitive equation model. In applying the scheme to flow on either the plane or the sphere, $\mathbf{r}(\tau + \Delta t)$ is assigned precisely using just the definitions of the grid points. For evaluating the higher derivatives in (1), no improvement is found in the present paper in going beyond simple centered finite differencing on the grid.

It is not obvious in advance how many terms should be retained in the Taylor series (1). Clearly this will depend on the spatial smoothness of the velocity field. Some guidelines are provided by the following error analysis, although a full examination is beyond the scope of this paper. Currently, only slight benefit has been found in going beyond the D_3 scheme. The scheme has been described above for two time-level applications; it can be modified in an obvious manner for three time-level applications.

b. *Operation counts*

The family of schemes proposed in (1), (2), and (4) represents a significant reduction in computing effort in the trajectory calculations. This is illustrated in Table 1 in the form of an operation count for typical calculations for a two-dimensional problem on the plane; a precalculation of common factors has been performed to minimize operation totals. For example, the D_3 scheme requires only nine additions and seven multiplications to compute either the x or y position of the departure point over a single time step. The calculations of (5) for $\hat{\mathbf{v}}$ are not included. By comparison,

TABLE 1. Typical operation counts for the D_1, D_2, D_3, and D_4 schemes used for calculating two-dimensional departure points (for each of the x and y components). Also shown are typical counts of a single biquadratic or bicubic interpolation, as would be used each iteration by competing schemes to update each advecting velocity component.

Scheme	Additions	Multiplications
D_1	1	1
D_2	5	4
D_3	9	7
D_4	13	10
Biquadratic interpolation	16	24
Bicubic interpolation	30	60

just a single interpolation of the bicubic interpolation for updating either u or v, as used by typical competing schemes, is considerably more expensive. Even the simpler biquadratic scheme has a relatively large count.

c. *Error analysis*

It is instructive to carry out an error analysis for the departure points for one-dimensional advection when there is only a single velocity component $u(x, t)$. For this purpose, an expression for the theoretical departure point is derived by using (1)–(3) without using approximation (4). This requires a general expression for the velocity at time $\tau + \Delta t$ in terms of the known velocities (presumed exact) at previous time steps. To achieve this, one may consider without loss of generality that $t = 0$ occurs at time $\tau + \Delta t/2$ and express the velocity $u(x, t)$ as an (Eulerian) Taylor series in t about this time,

$$u(x, t) = \hat{u}(x) + b_1(x)t + b_2(x)t^2 + O(t^3), \quad (6)$$

where formally

$$b_n(x) = \frac{1}{n!}\frac{\partial^n u}{\partial t^n}(\tau + \Delta t/2). \quad (7)$$

Here $\hat{u}$ may be derived by means of (5), which corresponds to setting $t = 0$ in (6); it can be seen that the third-order time accuracy of (6) is compatible with the time accuracy of the extrapolation formula (5). Defining the arrival point as $r(\tau + \Delta t) = x$, (6) may now be substituted into (1)–(3) to find an expansion for the theoretical departure point, namely, $r(\tau)$, where the rhs is to be evaluated at $t = \tau + \Delta t$, that is, $t = \Delta t/2$. Performing these substitutions (details are given in the Appendix) yields the final expression for the theoretical departure points

$$r(\tau) = x - \Delta t\hat{u} + \frac{\Delta t^2}{2}\hat{u}\frac{\partial \hat{u}}{\partial x} + \frac{\Delta t^3}{12}\left(b_1\frac{\partial \hat{u}}{\partial x} - \hat{u}\frac{\partial b_1}{\partial x} - b_2 - 2\hat{u}\frac{\partial}{\partial x}\hat{u}\frac{\partial \hat{u}}{\partial x}\right) + O(\Delta t^4). \quad (8)$$

One can now evaluate the accuracy of the presently proposed schemes. The D_1 scheme is identical to the first two terms of (8) and thus is accurate to $O(\Delta t)$. Thus, D_1 has similar accuracy to other first-order schemes such as that of Bates and McDonald (1982); the D_1 algorithm is similar to that scheme but differs in using a centered-in-time advecting velocity. As shown by Staniforth and Pudykiewicz (1985), such first-order schemes are inaccurate for large Courant numbers and exhibit poor conservation properties.

The D_2 scheme is identical to the first three terms of the theoretical expression (8) and is thus accurate to $O(\Delta t^2)$. This is the same as the accuracy of recent iterative centered-in-time schemes, as surveyed by Staniforth and Côté (1991).

The D_3 scheme is the same as the first four terms of (8), but only in the case that $b_1(x)$ and $b_2(x)$ are both zero. In general, these are nonzero and the D_3 scheme is only accurate to $O(\Delta t^2)$ with errors of order $O\{\Delta t^3[\partial^2 u/\partial t^2, \partial^2 u/\partial t\partial x, (\partial u/\partial t)(\partial u/\partial x)]\}$. The scheme is accurate to $O(\Delta t^3)$ in the case that the advecting velocity is steady in an Eulerian sense or that the indicated partial time derivatives of velocity vanish. Note that the D_3 and higher-order schemes actually calculate the $(\hat{u}\partial/\partial x)(\hat{u}\partial\hat{u}/\partial x)$ term, and thus in practice some reduction in error might be expected in using these schemes compared to the D_2 scheme. If the spatial derivatives of velocity are approximated by a simple centered formula, then the total error in the departure points is formally of order $O(\Delta t^3) + O(\Delta t^2\Delta x^2)$. If cubic interpolation is used to finally evaluate the model fields at these departure points, the resulting fields will have error of order $O(\Delta t^3) + O(\Delta t^2\Delta x^2) + O(\Delta x^4)$ per time step.

It is to be noted that the departure points have greater accuracy for the higher-order schemes in the case of the advecting velocity having small time or space derivatives. If the velocities also vary approximately linearly in space, then the truncation errors will be further reduced for the spatial finite differencing. This explains why it is particularly advantageous to evaluate the higher-order terms for the steady examples shown in sections 3 and 4 of this paper. For a velocity field that is noisy or shows high variability in space or time, (8) indicates there may be little advantage in going beyond a D_2 scheme; as in this case, the higher-order schemes will possess similar truncation errors to the D_2 scheme.

In typical semi-implicit semi-Lagrangian schemes, the primitive equations are manipulated to form time averages of terms at the arrival and departure points. This averaging restricts the time accuracy of the fields to $O(\Delta t^3)$ over one time step when those fields are known precisely at the departure points. When the D_2 scheme is incorporated, this provides a net second-order accuracy with the same truncation errors as given above. These estimates are similar to the accuracy of schemes such as those discussed by McDonald (1987), where $\hat{u}$ is centered in both space and time.

d. Calculations on the sphere

For fluid flow on the surface of a sphere with (longitude, latitude, radius) = (λ, θ, a), the operator $\hat{\mathbf{v}} \cdot \nabla$ may be expressed as

$$\hat{\mathbf{v}} \cdot \nabla \equiv \frac{\hat{u}}{a \cos\theta} \frac{\partial}{\partial \lambda} + \frac{\hat{v}}{a} \frac{\partial}{\partial \theta}. \quad (9)$$

The (λ, θ) velocity components $\hat{u}$ and $\hat{v}$ are to be evaluated at time $\tau + \Delta t/2$. The position vectors are most conveniently expressed in Cartesian coordinates to ensure that they smoothly vary near the poles, a technique used by Ritchie (1987). A typical arrival point may be written as

$$\mathbf{r}(\tau + \Delta t) = (X, Y, Z)_a$$
$$= (a \cos\lambda_a \cos\theta_a, a \sin\lambda_a \cos\theta_a, a \sin\theta_a), \quad (10)$$

with velocity components in the directions of the Cartesian coordinate axes given by

$$\frac{d\mathbf{r}(\tau + \Delta t)}{dt} = (\dot{X}, \dot{Y}, \dot{Z})_a \approx \hat{\mathbf{v}} \cdot \nabla (X, Y, Z)_a, \quad (11)$$

where the approximation of (4) has been invoked. Applying (9) gives

$$\frac{d\mathbf{r}(\tau + \Delta t)}{dt} \approx (-\hat{u} \sin\lambda_a - \hat{v} \cos\lambda_a \sin\theta_a,$$
$$\hat{u} \cos\lambda_a - \hat{v} \sin\lambda_a \sin\theta_a, \hat{v} \cos\theta_a). \quad (12)$$

The same rhs velocity components could have been obtained alternatively by trigonometry. The higher-order terms in (1) may be evaluated by repeatedly applying the operator (9). In the present paper, this is performed by means of simple centered finite differencing on the regular polar-coordinate grid. The X-, Y-, and Z-component calculations are independent of one another. Note that the functions being differentiated by (9) vary smoothly across the poles, and the derivatives are easily evaluated by finite differences after extending the arrays beyond $\theta = 0$ and $\theta = \pi$ in the manner described below for other scalar quantities.

The terms in (1) may be summed to give $\mathbf{r}(\tau)$ denoted here by (X, Y, Z). The equivalent values of (λ, θ) may then be calculated from (X, Y, Z) using the inverse form of (10) to return to spherical polar coordinates, namely,

$$\lambda = \text{ATAN2}(Y, X) \quad (13)$$

$$\theta = \arcsin[Z(X^2 + Y^2 + Z^2)^{-1/2}], \quad (14)$$

where ATAN2 denotes the Fortran arctan function with double arguments. The radial component could also have been evaluated, which would not in general equal the arrival point value of a, the sphere's radius. The procedure of ignoring the variation of the radial component is equivalent to taking the projection of vector $\mathbf{r}(\tau)$ on the sphere's surface as the departure point. Note again that expressing the position vectors in Cartesian coordinates has avoided any problems at the poles and that the polar form of the departure points automatically lie in a sensible range of values by virtue of (13) and (14), with $0 \leq \lambda < 2\pi$ and $-\pi < \theta \leq \pi$.

Required field values may then be obtained from interpolation in (λ, θ) space, for example, using bicubic interpolation. Alternatively, having obtained the departure points as described above, they could also be used for a "noninterpolating" advective scheme in the manner described by Ritchie (1987); this option has not been pursued in the present study. In order to perform bicubic interpolations, it can be seen that the interpolating arrays typically need to be extended cyclically one column to the west and two columns to the east. They also need to be extended beyond the poles two rows north and two rows south by repeating the values of the nearest two rows but incorporating a longitudinal phase shift of π to allow for crossing the poles; this assumes the grid points have been set up so as not to actually coincide with the poles. If vector quantities are being interpolated, then the vector sign must also be reversed for these north–south extensions.

3. Steady two-dimensional flow—The cone test

The scheme described by (1)–(4) was applied to a form of the cone test of Crowley (1968) for a range of time steps. The domain has 33×33 grid points covering $-16 \leq x \leq 16$, $-16 \leq y \leq 16$. The cone has initial height $\phi = 100$ units, the diameter of its base is 8 grid units, and it is initially centered at $(-8, 0)$. These are the same settings as used by McDonald (1984); this includes a buffer of one row around the lateral boundary in which the height is held at zero. Table 2 shows the errors for various order schemes after one clockwise cycle of solid-body rotation about the origin; results using theoretical departure points are also listed. Figure 1a shows the initial conditions and Figs. 1b and 1c show the height after one revolution using the D_3 scheme for the cases of 288 and 48 steps per revolution, respectively. The positions and symmetry of the cone are excellent for this scheme, although some smoothing of the profile is evident, particularly for the smaller time steps.

The table shows that the departure point calculation is extremely accurate for the D_3 or D_4 scheme. This accuracy is related to the precise determination of the horizontal derivatives in (4) for this problem—the cone test has steady velocities that are linear in x and y; thus, the second and higher total time derivatives of the position vectors are also linear in x and y and are determined exactly by the finite differencing.

The accuracy can be further demonstrated by writing out the series expansion for the trajectories for the present case of steady two-dimensional solid-body rotation with $\mathbf{v} = (\Omega y, -\Omega x)$ and correspondingly $\mathbf{v} \cdot \nabla = \Omega y \partial/\partial x - \Omega x \partial/\partial y$. Then, for $\mathbf{r}(\tau + \Delta t) = (x, y)$, the theoretical solution for $\mathbf{r}(\tau)$ from (1) is

TABLE 2. Maximum height, minimum height, radial error in units of grid lengths, angular error in degrees, and conservation properties after one revolution of the cone test are shown. Several schemes are shown for calculating the departure points for a variety of time-step sizes; all schemes use bicubic interpolation. Initially the maximum height is 100 and the minimum is zero.

Number of steps	Maximum height	Minimum height	Radial error	Angular error	$\frac{\Sigma \phi_{ij}}{\Sigma \phi_{ij}(0)}$	$\frac{\Sigma \phi_{ij}^2}{\Sigma \phi_{ij}^2(0)}$
D_1 scheme						
288	55	−3	−1.0	−1°	0.874	0.58
48	60	−2	−2.7	−1°	0.442	0.32
24	56	−2	−4.3	−7°	0.204	0.14
16	44	−2	−5.5	−20°	0.101	0.06
D_2 scheme						
288	57	−2	−0.1	−1°	1.005	0.68
48	75	−2	0.0	1°	0.997	0.85
24	80	−1	−0.1	4°	0.973	0.88
16	82	−1	−0.4	9°	0.909	0.84
D_3 scheme						
288	57	−2	−0.1	−1°	1.005	0.68
48	75	−2	0.0	0°	1.002	0.85
24	80	−2	0.0	0°	1.010	0.92
16	82	−1	0.1	0°	1.030	0.96
D_4 scheme						
288	57	−2	−0.1	−1°	1.005	0.68
48	75	−2	0.0	0°	1.000	0.85
24	80	−2	0.0	0°	1.000	0.91
16	82	−1	0.0	0°	1.000	0.93
Using theoretical departure points						
288	57	−2	−0.1	−1°	1.005	0.68
48	75	−2	0.0	0°	1.000	0.85
24	80	−2	0.0	0°	1.000	0.91
16	82	−1	0.0	0°	1.000	0.93

$$\mathbf{r}(\tau) = (x - \Delta t\Omega y - \Delta t^2\Omega^2 x/2 + \Delta t^3\Omega^3 y/6 + \cdots,$$
$$y - \Delta t\Omega x - \Delta t^2\Omega^2 y/2 - \Delta t^3\Omega^3 x/6 + \cdots). \quad (15)$$

Thus, the $D_1, D_2, D_3, \ldots$ schemes agree precisely with (15) for 2, 3, 4, ... terms, respectively, taken in the series. It can be seen that the present family of schemes are capable of arbitrary order accuracy in calculating departure points for the cone test.

As expected, the most accurate results occur for the D_4 scheme, which is indistinguishable from the calculation with theoretical departure points (for the number of digits displayed). Its small improvement over the D_3 scheme is seen in regard to "mass" conservation for larger time steps. The D_3 scheme produces superior results to the D_2 scheme in respect to reduced angular error and improved conservation properties. It may be noted that the results for the D_1 scheme are the same as those of McDonald's (1984) iterative scheme for departure points; both schemes use bicubic interpolation but are first order in time. Table 2 verifies the poor conservation properties of such first-order schemes, as reported by Staniforth and Pudykiewicz (1985).

In common with the results shown by McDonald (1984) for theoretical departure points, the height errors for the higher-order schemes are least when larger time steps are used; this may be ascribed to the smaller number of interpolations then performed each revolution. Results for the same cone test were given by McGregor (1987) for several horizontally split advection schemes; the split-cubic scheme produced similar errors to the present D_2 scheme.

4. Steady flow on a sphere—Ritchie's test

Ritchie (1987) proposed a test problem of a "Gaussian hill" on a sphere. The center of the hill is located initially on the equator at (0°, 0°), with its height satisfying a Gaussian profile when viewed from a stereographic projection true at (longitude, latitude) = (0°, 45°). The peak height is prescribed as 100 units, and the profile is defined such that a length L represents approximately the diameter at which the height equals

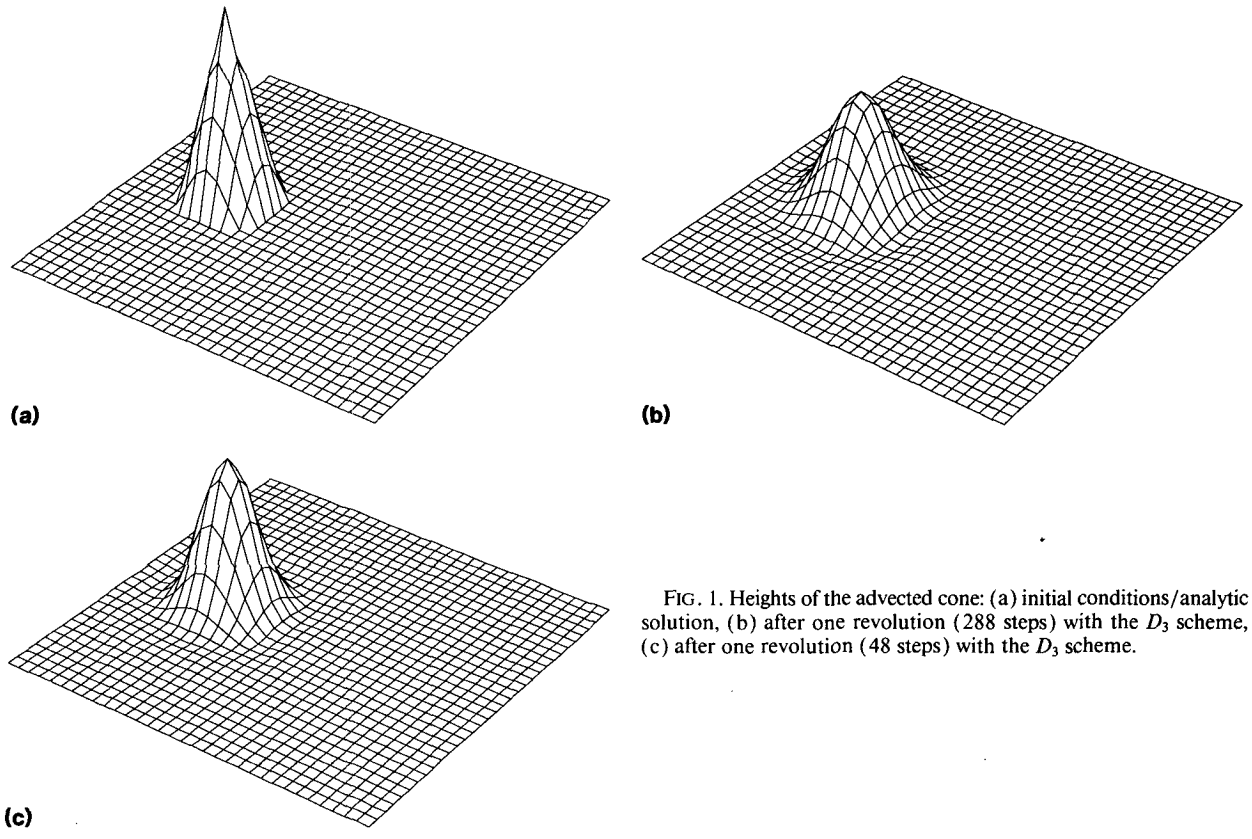

FIG. 1. Heights of the advected cone: (a) initial conditions/analytic solution, (b) after one revolution (288 steps) with the D_3 scheme, (c) after one revolution (48 steps) with the D_3 scheme.

10 units. More details of this initial height prescription are given by Ritchie (1987). The stereographic projection only arises in assigning the initial height field. Figures 2 and 3a show the initial Gaussian hills for L = 10 000 and 2500 km, respectively, displayed on a simple longitude–latitude projection.

An advecting velocity corresponding to steady solid-body rotation of one rotation per 20 days is prescribed, with the axis of rotation passing through the middle of the sphere and the point $(\lambda_0, \theta_0) = (0°, 45°)$,

$$u = a\omega[\cos\theta \sin\theta_0 - \cos(\lambda - \lambda_0) \sin\theta \cos\theta_0] \quad (16)$$

$$v = a\omega \sin(\lambda - \lambda_0) \cos\theta_0. \quad (17)$$

This velocity field should advect the Gaussian hill without deformation from its position on the equator in a counterclockwise circular sense over the North Pole and back again to its original position on the equator in 20 days. Ritchie used a leapfrog time-differencing scheme with a time step of 6 h, thereby proceeding in decoupled 12-h leaps; to provide a proper comparison for the present two-time-level scheme, a time step of 12 h is used.

a. Calculations on a Gaussian grid

The present scheme and Ritchie's scheme both use bicubic interpolation on a Gaussian grid with resolution appropriate to a T42 spectral model. Similar to Ritchie, all variables are held in (λ, θ) arrays, with K_1 = 128 longitude values and K_2 = 64 latitude values. The longitudes are given by

$$\lambda_i = \frac{2\pi(i-1)}{K_1} - \pi, \quad 1 \leq i \leq K_1, \quad (18)$$

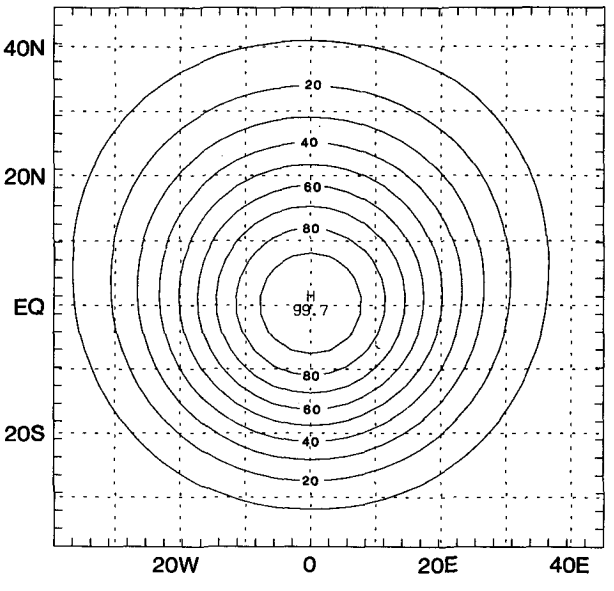

FIG. 2. Initial condition height contours for the "Gaussian hill" advection test on the sphere for L = 10 000 km. Latitudes and longitudes are shown. Tick marks represent the grid spacing.

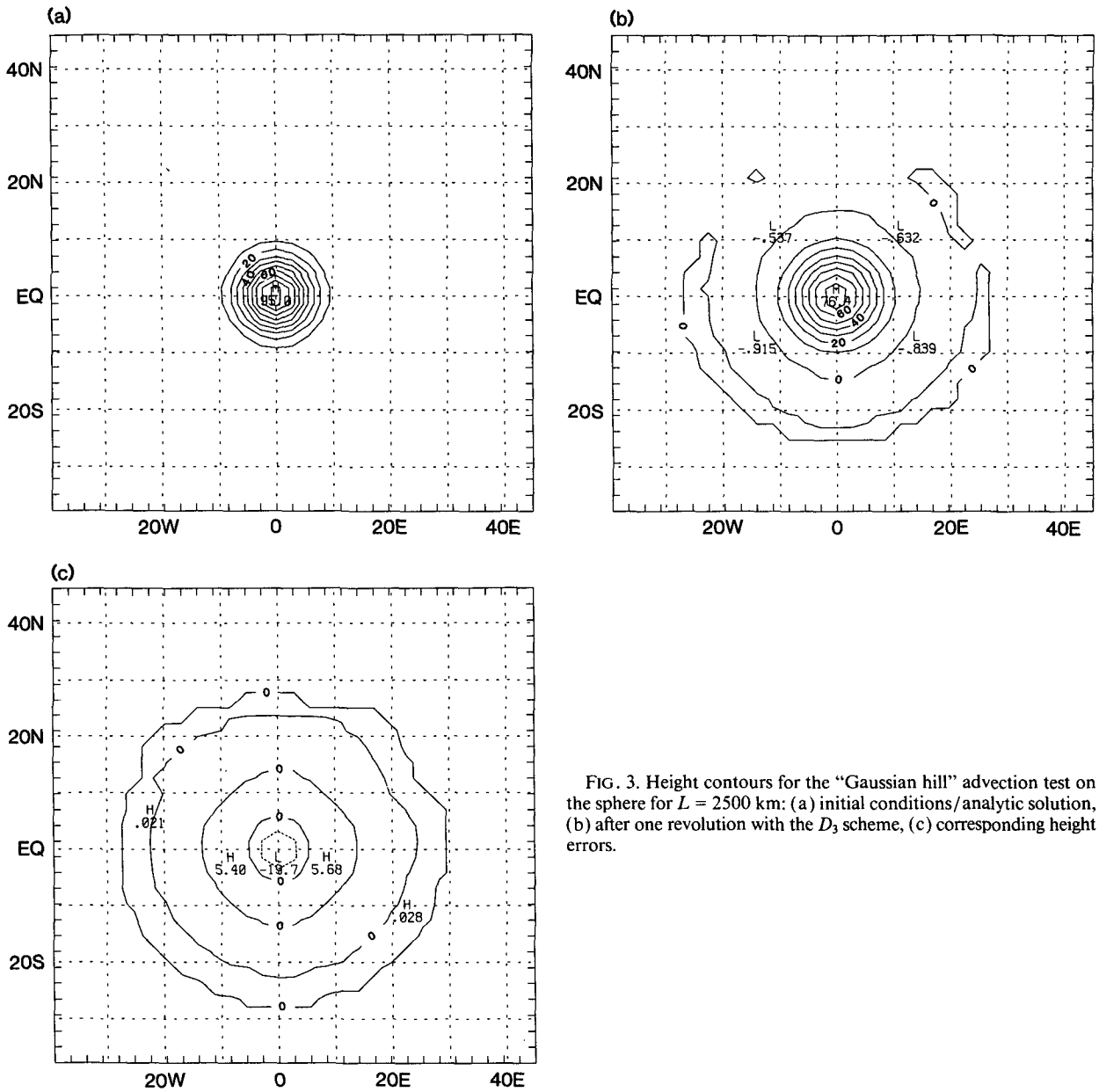

FIG. 3. Height contours for the "Gaussian hill" advection test on the sphere for $L = 2500$ km: (a) initial conditions/analytic solution, (b) after one revolution with the D_3 scheme, (c) corresponding height errors.

and the Gaussian latitudes are well approximated by

$$\theta_j = \frac{(2j - K_2 - 1)\pi}{2K_2 + 1}, \quad 1 \leq j \leq K_2, \qquad (19)$$

although the precise values were actually used. Calculations were performed using the scheme (1)–(4) truncating at either the second, third, or fourth total time derivative, namely, D_2, D_3, and D_4 versions of the scheme. An example is shown in Figs. 3a and 3b for the D_3 scheme applied to the case $L = 2500$ km after one rotation (40 steps or 20 days integration); the plotting program has reduced the peak of the initial pattern from 100 units because the peak is located between grid points. The height errors are plotted in Fig. 3c. The results are fairly similar to those given by Ritchie (1987) for this case (compare his Fig. 10) and are superior to the standard Eulerian spectral calculation (leapfrog time step of 1.5 h) also shown in his paper. Table 3 summarizes the results for a range of values of length L, during one rotation. In the table, the error denotes the area integral of the absolute value of the errors expressed as a percentage of the area integral of the analytic solution.

The present scheme has greatest accuracy for larger values of L, as is the case for all the other schemes. Since for the present scheme and for Ritchie's interpolating scheme the departure displacements do not vary from one time step to another, nor from one choice of Gaussian hill to another, this suggests a more

TABLE 3. Percentage errors for one-fourth, one-half, three-fourths, and one revolution of the "Gaussian hill" advection problem. Models D_2, D_3, and D_4 give results for the present scheme with Δt = 12 h. Ritchie I, Ritchie N, and Eulerian denote values from Ritchie's (1987) paper with Δt = 6 h; "I" denotes interpolating, "N" denotes non-interpolating. Theoretical departure point is denoted as theor. d.p. The most accurate result for each length L is denoted by *.

L (km)	Model	Prognosis period (h) 120	240	360	480
10 000	Eulerian	0.22	0.34	0.55	0.68
10 000	Ritchie I	0.18	0.35	0.52	0.70
10 000	Ritchie N	0.31	0.55	0.77	1.01
10 000	D_2	1.14	2.28	3.43	4.57
10 000	D_3	0.05	0.09	0.13	0.18
10 000	D_4	0.04*	0.07*	0.10*	0.14*
10 000	Theor. d.p.	0.04	0.07	0.10	0.14
5000	Eulerian	1.55	2.73	4.24	5.48
5000	Ritchie I	0.57*	0.96*	1.36	1.90
5000	Ritchie N	0.62	1.05	1.31*	1.67*
5000	D_2	2.44	4.77	7.22	9.63
5000	D_3	0.58	0.92	1.28	1.80
5000	D_4	0.58	0.91	1.26	1.77
5000	Theor. d.p.	0.58	0.91	1.26	1.77
2500	Eulerian	15.2	26.4	38.0	48.2
2500	Ritchie I	6.31	8.02	10.6	15.2
2500	Ritchie N	4.71*	6.44*	8.08*	9.72*
2500	D_2	8.68	13.44	18.99	25.89
2500	D_3	7.55	10.56	14.39	19.63
2500	D_4	7.54	10.54	14.38	19.60
2500	Theor. d.p.	7.54	10.55	14.38	19.61

accurate evaluation of the departure points than in Ritchie's scheme. In fact, Table 3 shows that the D_4 scheme produces results virtually indistinguishable from the calculation with theoretical departure points. Ritchie's greater accuracy for small L (with his comparable interpolating version) indicates that he has managed to implement a more accurate bicubic algorithm for his final interpolations.

It may be noted that in the present case of solid-body rotation, the Cartesian components of the velocity and each total time derivative may be written as linear combinations of X, Y, and Z; this may be seen by noting the effect of repeated application of the $\mathbf{v}\cdot\nabla$ operator. There would then be no spatial truncation errors if operator (4) could be applied by Cartesian finite differencing. Although the derivatives may not be precisely evaluated during finite differencing in polar coordinates, spatial truncation errors will still be small. Coupled with the steadiness of the advection velocity, the accuracy analysis of section 2 indicates the scheme should be at least third-order accurate because the Δt^3 terms in (8) are being evaluated accurately. This then explains the benefits of the higher-order schemes over the D_2 scheme for this problem.

b. Calculations on a regular grid

The above advection calculations on the sphere were repeated with the prescription for the gridpoint latitudes (19) replaced by an equally spaced set of values

$$\theta_j = \frac{(2j - K_2 - 1)\pi}{2K_2}, \quad 1 \leqslant j \leqslant K_2 \qquad (20)$$

as might be employed in a gridpoint prediction model. This expression permits a simpler formula for the bicubic interpolations. Table 4 displays the results of the calculations repeated on the regular grid; there is a slight decrease in accuracy compared to the Gaussian grid.

c. Accuracy of the departure points

For the above solid-body rotation problem, it is possible to write down exact expressions for the departure point of each grid point over a time step. An expression for the rms fractional trajectory errors over the sphere is given by

$$(\text{rmse})^2 = \frac{\sum w|\mathbf{r} - \mathbf{r}_{\text{theor}}|^2}{\sum w|\mathbf{r} - \mathbf{r}_a|^2}, \qquad (21)$$

where the summations are over all grid points, and w is a weight proportional to the area of a grid square. Also, $\mathbf{r}_a$ denotes an arrival vector grid position, $\mathbf{r}$ denotes the calculated departure point, and $\mathbf{r}_{\text{theor}}$ denotes the theoretical departure point. Table 5 shows the errors expressed as percentages for computations with various order schemes using a 12-h time step. The summations are most conveniently calculated in Cartesian coordinates. The D_1 scheme clearly has excessive errors of about 4% each time step for the trajectories; this scheme corresponds to just using straight-line trajectories determined solely by the arrival-point velocity vectors. The errors steadily decrease to better than 2 parts in 10^5 for the D_4 scheme. When higher-order schemes up to D_8 are used, the errors do not change from the D_4 values (with 64-bit arithmetic); with even higher-order schemes, the errors slowly increase as rounding errors become significant.

TABLE 4. Percentage errors for one-fourth, one-half, three-fourths, and one revolution of the "Gaussian hill" advection problem, as in Table 3 but with the calculations performed on a grid that is uniformly spaced latitudinally.

L (km)	Model	Prognosis period (h) 120	240	360	480
10 000	D_2	1.14	2.28	3.43	4.58
10 000	D_3	0.05	0.09	0.13	0.18
10 000	D_4	0.04	0.07	0.10	0.14
5000	D_2	2.45	4.76	7.22	9.63
5000	D_3	0.60	0.93	1.29	1.82
5000	D_4	0.59	0.92	1.27	1.79
2500	D_2	8.81	13.48	19.10	26.02
2500	D_3	7.77	11.19	14.39	19.68
2500	D_4	7.77	11.18	14.37	19.65

TABLE 5. Root-mean-square percentage trajectory errors per time step on the sphere for the solid-body rotation problem and $\Delta t = 12$ h. The errors are the same whether Gaussian latitudes or equally spaced latitudes are used.

Scheme	Percentage trajectory errors
D_1	3.6
D_2	0.41
D_3	0.006
D_4	0.0015

d. Analytic evaluation of the horizontal derivatives

In the context of a spectral model, it is possible to evaluate horizontal derivatives more accurately than the finite differencing used above. To obtain an indication of the impact of this higher accuracy, the experiment (a) above was repeated with analytic expressions for the second total time derivative terms. Separate results are not shown because they differ from the corresponding results in Table 3 only to the extent of rounding error in the last significant figure shown. This result supports the contention that the present method will accurately determine the departure points, at least for an advecting velocity field that varies smoothly in space and time.

5. Conclusions

A family of efficient schemes for determining the departure points of fluid parcels has been proposed and evaluated. The schemes utilize the parcel velocity and Eulerian estimates of its first and second material derivative (in the case of the D_3 scheme), resulting in a departure vector expressed as a truncated Taylor series. An operation count was used to show that the computational effort is less than that of other schemes of comparable accuracy, where typically horizontal interpolation is used to find iterative corrections to the advecting velocities. On the sphere, the computational savings of the present schemes become more pronounced; in this case, trigonometric Cartesian-to-polar conversions are avoided during the intermediate calculations of the departure points.

The accuracy of the present schemes has been shown to be at least comparable to other schemes for the examples of the cone test on the plane and Ritchie's "Gaussian hill" problem on the rotating sphere. For both the cone test and Ritchie's test, the results for the D_4 scheme were best in that they were essentially indistinguishable from those using theoretical departure points.

This paper has not fully addressed the problems associated with time-dependent advecting velocities. The D_2 scheme has similar time truncation errors to recent iterative centered-in-time schemes. The error analysis revealed that the higher-order schemes possess smaller time truncation errors when the advecting velocities do not exhibit high variability in space or time. The D_3 scheme has been incorporated sucessfully into a semi-Lagrangian limited-area primitive equation model.

Acknowledgments. Improvements to the manuscript were suggested by Martin Dix and Drs. Mukut Mathur, Michael Naughton, and Andrew Staniforth.

APPENDIX

Extra Details for the Error Analysis

This appendix provides details of the algebra when (6) is substituted into (1)–(3) to obtain the theoretical departure point for a one-dimensional problem. Equations (1)–(3) may be expanded as

$$r(\tau) = x - \Delta t u + \frac{\Delta t^2}{2!}\left(\frac{\partial u}{\partial t} + u\frac{\partial u}{\partial x}\right) - \frac{\Delta t^3}{3!}\left(\frac{\partial}{\partial t} + u\frac{\partial}{\partial x}\right)\left(\frac{\partial u}{\partial t} + u\frac{\partial u}{\partial x}\right) + O(\Delta t^4), \quad \text{(A1)}$$

where the rhs is to be evaluated at time $\tau + \Delta t$. The terms may be regrouped as

$$r(\tau) = x - \Delta t u + \frac{\Delta t^2}{12}\left(6 - 2\Delta t\frac{\partial}{\partial t} - 2\Delta t u\frac{\partial}{\partial x}\right) \times \left(\frac{\partial u}{\partial t} + u\frac{\partial u}{\partial x}\right) + O(\Delta t^4). \quad \text{(A2)}$$

Substituting u from (6) and retaining only terms up to $O(\Delta t^3)$, which requires an appreciation that the rhs is to be evaluated for $t = \Delta t/2$, gives

$$r(\tau) = x - \Delta t(\hat{u} + b_1 t + b_2 t^2) + \frac{\Delta t^2}{12}\left(6 - 2\Delta t\frac{\partial}{\partial t} - 2\Delta t\hat{u}\frac{\partial}{\partial x}\right)\left[b_1 + 2b_2 t + \hat{u}\frac{\partial \hat{u}}{\partial x} + \frac{\partial}{\partial x}(\hat{u}b_1)t\right] + O(\Delta t^4). \quad \text{(A3)}$$

Performing the remaining derivatives and continuing to retain only terms up to $O(\Delta t^3)$ gives

$$r(\tau) = x - \Delta t(\hat{u} + b_1 t + b_2 t^2) + \frac{\Delta t^2}{12}\left\{6\left[b_1 + 2b_2 t + \hat{u}\frac{\partial \hat{u}}{\partial x} + \frac{\partial}{\partial x}(\hat{u}b_1)t\right] - 2\Delta t\left[2b_2 + \frac{\partial}{\partial x}(\hat{u}b_1)\right] - 2\Delta t\left(\hat{u}\frac{\partial b_1}{\partial x} + \hat{u}\frac{\partial}{\partial x}\hat{u}\frac{\partial \hat{u}}{\partial x}\right)\right\} + O(\Delta t^4). \quad \text{(A4)}$$

Substituting $t = \Delta t/2$ yields

$$r(\tau) = x - \Delta t\left(\hat{u} + b_1\frac{\Delta t}{2} + b_2\frac{\Delta t^2}{4}\right) + \frac{\Delta t^2}{12}\left[6b_1 + 6b_2\Delta t + 6\hat{u}\frac{\partial \hat{u}}{\partial x} + 3\frac{\partial}{\partial x}(\hat{u}b_1)\Delta t\right.$$
$$\left. - 4b_2\Delta t - 2\frac{\partial}{\partial x}(\hat{u}b_1)\Delta t - 2\hat{u}\frac{\partial b_1}{\partial x}\Delta t - 2\hat{u}\frac{\partial}{\partial x}\hat{u}\frac{\partial \hat{u}}{\partial x}\Delta t\right] + O(\Delta t^4). \quad \text{(A5)}$$

Equation (8) now follows directly by collecting the terms together.

REFERENCES

Bates, J. R., and A. McDonald, 1982: Multiply-upstream, semi-Lagrangian advective schemes: Analysis and application to a multilevel primitive equation model. *Mon. Wea. Rev.*, **110,** 1831–1842.

——, F. H. M. Semazzi, R. W. Higgins, and S. R. M. Barros, 1990: Integration of the shallow water equations on the sphere using a vector semi-Lagrangian scheme with a multigrid solver. *Mon. Wea. Rev.*, **118,** 1615–1627.

Crowley, W. P., 1968: Numerical advection experiments. *Mon. Wea. Rev.*, **96,** 1–11.

McDonald, A., 1984: Accuracy of multiply-upstream, semi-Lagrangian advective schemes. *Mon. Wea. Rev.*, **112,** 1267–1275.

——, 1986: A semi-Lagrangian and semi-implicit two time-level integration scheme. *Mon. Wea. Rev.*, **114,** 824–830.

——, 1987: Accuracy of multiply-upstream, semi-Lagrangian advective schemes II. *Mon. Wea. Rev.*, **115,** 1446–1450.

——, and J. R. Bates, 1987: Improving the estimate of the departure point position in a two-time-level semi-Lagrangian and semi-implicit model. *Mon. Wea. Rev.*, **115,** 737–739.

——, and ——, 1989: Semi-Lagrangian integration of a gridpoint shallow water model on the sphere. *Mon. Wea. Rev.*, **117,** 130–137.

McGregor, J. L., 1987: Accuracy and initialization of a two-time-level semi-Lagrangian model. *Short- and Medium-Range Numerical Weather Prediction,* T. Matsuno, Ed., Special Volume of the J. Meteor. Soc. Japan, 233–246.

Mathur, M. B., 1970: A note on an improved quasi-Lagrangian advective scheme for primitive equations. *Mon. Wea. Rev.*, **98,** 214–219.

Ritchie, H., 1987: Semi-Lagrangian advection on a Gaussian grid. *Mon. Wea. Rev.*, **115,** 608–619.

Robert, A., 1981: A stable numerical integration scheme for the primitive meteorological equations. *Atmos.-Ocean,* **19,** 35–46.

——, 1982: A semi-Lagrangian and semi-implicit numerical integration scheme for the primitive meteorological equations. *J. Meteor. Soc. Japan,* **60,** 319–325.

Staniforth, A., and J. Pudykiewicz, 1985: Reply to comments on and addenda to "Some properties and comparative performance of the semi-Lagrangian method of Robert in the solution of the advection-diffusion equation." *Atmos.-Ocean,* **23,** 195–200.

——, and J. Côté, 1991: Semi-Lagrangian integration schemes for atmospheric models—A review. *Mon. Wea. Rev.*, **119,** 2206–2223.

Tanguay, M., A. Simard, and A. Staniforth, 1989: A three-dimensional semi-Lagrangian scheme for the Canadian regional finite-element forecast model. *Mon. Wea. Rev.*, **117,** 1861–1871.

Temperton, C., and A. Staniforth, 1987: An efficient two-time-level semi-Lagrangian semi-implicit integration scheme. *Quart. J. Roy. Meteor. Soc.* **113,** 1025–1039.

Williamson, D. L., and P. J. Rasch, 1989: Two-dimensional semi-Lagrangian transport with shape-preserving interpolation. *Mon. Wea. Rev.*, **117,** 102–129.